BELLE-CONF-0822
BELLE Preprint 2009-7
KEK Preprint 2008-56

Measurement of the Differential Branching Fraction and Forward-Backward Asymmetry for $B \to K^{(*)}\ell^+\ell^-$

J.-T. Wei,[25] P. Chang,[25] I. Adachi,[8] H. Aihara,[41] V. Aulchenko,[1,30] T. Aushev,[17,12] A. M. Bakich,[37] V. Balagura,[12] E. Barberio,[20] A. Bondar,[1,30] A. Bozek,[26] M. Bračko,[19,13] T. E. Browder,[7] Y.-W. Chang,[25] Y. Chao,[25] A. Chen,[23] K.-F. Chen,[25] B. G. Cheon,[6] C.-C. Chiang,[25] I.-S. Cho,[45] Y. Choi,[36] J. Dalseno,[8] A. Drutskoy,[2] W. Dungel,[10] S. Eidelman,[1,30] N. Gabyshev,[1,30] P. Goldenzweig,[2] B. Golob,[18,13] H. Ha,[15] B.-Y. Han,[15] K. Hayasaka,[21] H. Hayashii,[22] M. Hazumi,[8] Y. Horii,[40] Y. Hoshi,[39] W.-S. Hou,[25] H. J. Hyun,[16] T. Iijima,[21] K. Inami,[21] R. Itoh,[8] M. Iwasaki,[41] Y. Iwasaki,[8] D. H. Kah,[16] H. Kaji,[21] J. H. Kang,[45] P. Kapusta,[26] N. Katayama,[8] T. Kawasaki,[28] H. Kichimi,[8] H. J. Kim,[16] H. O. Kim,[16] S. K. Kim,[35] Y. I. Kim,[16] Y. J. Kim,[5] K. Kinoshita,[2] B. R. Ko,[15] S. Korpar,[19,13] P. Križan,[18,13] P. Krokovny,[8] A. Kuzmin,[1,30] Y.-J. Kwon,[45] S.-H. Kyeong,[45] J. S. Lange,[4] M. J. Lee,[35] S. E. Lee,[35] T. Lesiak,[26,3] J. Li,[7] A. Limosani,[20] C. Liu,[34] D. Liventsev,[12] R. Louvot,[17] F. Mandl,[10] A. Matyja,[26] S. McOnie,[37] T. Medvedeva,[12] K. Miyabayashi,[22] H. Miyata,[28] Y. Miyazaki,[21] R. Mizuk,[12] E. Nakano,[31] M. Nakao,[8] H. Nakazawa,[23] Z. Natkaniec,[26] S. Nishida,[8] K. Nishimura,[7] O. Nitoh,[43] T. Nozaki,[8] S. Ogawa,[38] T. Ohshima,[21] S. Okuno,[14] H. Ozaki,[8] G. Pakhlova,[12] C. W. Park,[36] H. Park,[16] H. K. Park,[16] K. S. Park,[36] L. E. Piilonen,[44] M. Rozanska,[26] H. Sahoo,[7] K. Sakai,[28] Y. Sakai,[8] O. Schneider,[17] C. Schwanda,[10] A. J. Schwartz,[2] R. Seidl,[32] A. Sekiya,[22] K. Senyo,[21] M. E. Sevior,[20] M. Shapkin,[11] C. P. Shen,[7] J.-G. Shiu,[25] B. Shwartz,[1,30] S. Stanič,[29] M. Starič,[13] T. Sumiyoshi,[42] S. Suzuki,[33] M. Tanaka,[8] G. N. Taylor,[20] Y. Teramoto,[31] K. Trabelsi,[8] S. Uehara,[8] T. Uglov,[12] Y. Unno,[6] S. Uno,[8] P. Urquijo,[20] Y. Usov,[1,30] G. Varner,[7] K. E. Varvell,[37] K. Vervink,[17] C. C. Wang,[25] C. H. Wang,[24] M.-Z. Wang,[25] P. Wang,[9] X. L. Wang,[9] Y. Watanabe,[14] R. Wedd,[20] J. Wicht,[8] E. Won,[15] B. D. Yabsley,[37] Y. Yamashita,[27] M. Yamauchi,[8] C. Z. Yuan,[9] Z. P. Zhang,[34] T. Zivko,[13] A. Zupanc,[13] and O. Zyukova[1,30]

(The Belle Collaboration)

[1]*Budker Institute of Nuclear Physics, Novosibirsk*
[2]*University of Cincinnati, Cincinnati, Ohio 45221*
[3]*T. Kościuszko Cracow University of Technology, Krakow*
[4]*Justus-Liebig-Universität Gießen, Gießen*
[5]*The Graduate University for Advanced Studies, Hayama*
[6]*Hanyang University, Seoul*
[7]*University of Hawaii, Honolulu, Hawaii 96822*
[8]*High Energy Accelerator Research Organization (KEK), Tsukuba*
[9]*Institute of High Energy Physics, Chinese Academy of Sciences, Beijing*
[10]*Institute of High Energy Physics, Vienna*
[11]*Institute of High Energy Physics, Protvino*
[12]*Institute for Theoretical and Experimental Physics, Moscow*
[13]*J. Stefan Institute, Ljubljana*
[14]*Kanagawa University, Yokohama*

[15]Korea University, Seoul
[16]Kyungpook National University, Taegu
[17]École Polytechnique Fédérale de Lausanne (EPFL), Lausanne
[18]Faculty of Mathematics and Physics, University of Ljubljana, Ljubljana
[19]University of Maribor, Maribor
[20]University of Melbourne, School of Physics, Victoria 3010
[21]Nagoya University, Nagoya
[22]Nara Women's University, Nara
[23]National Central University, Chung-li
[24]National United University, Miao Li
[25]Department of Physics, National Taiwan University, Taipei
[26]H. Niewodniczanski Institute of Nuclear Physics, Krakow
[27]Nippon Dental University, Niigata
[28]Niigata University, Niigata
[29]University of Nova Gorica, Nova Gorica
[30]Novosibirsk State University, Novosibirsk
[31]Osaka City University, Osaka
[32]RIKEN BNL Research Center, Upton, New York 11973
[33]Saga University, Saga
[34]University of Science and Technology of China, Hefei
[35]Seoul National University, Seoul
[36]Sungkyunkwan University, Suwon
[37]University of Sydney, Sydney, New South Wales
[38]Toho University, Funabashi
[39]Tohoku Gakuin University, Tagajo
[40]Tohoku University, Sendai
[41]Department of Physics, University of Tokyo, Tokyo
[42]Tokyo Metropolitan University, Tokyo
[43]Tokyo University of Agriculture and Technology, Tokyo
[44]IPNAS, Virginia Polytechnic Institute and State University, Blacksburg, Virginia 24061
[45]Yonsei University, Seoul

Abstract

We study $B \to K^{(*)}\ell^+\ell^-$ decays ($\ell = e, \mu$) based on a data sample of 657 million $B\overline{B}$ pairs collected with the Belle detector at the KEKB e^+e^- collider. We report the differential branching fraction, isospin asymmetry, K^* polarization, and the forward-backward asymmetry (A_{FB}) as functions of $q^2 = M^2_{\ell\ell}c^2$. The fitted A_{FB} spectrum exceeds the Standard Model expectation by 2.7 standard deviations. The measured branching fractions are $\mathcal{B}(B \to K^*\ell^+\ell^-) = (10.7^{+1.1}_{-1.0} \pm 0.9) \times 10^{-7}$ and $\mathcal{B}(B \to K\ell^+\ell^-) = (4.8^{+0.5}_{-0.4} \pm 0.3) \times 10^{-7}$, where the first errors are statistical and the second are systematic, with the muon to electron ratios $R_{K^*} = 0.83 \pm 0.17 \pm 0.08$ and $R_K = 1.03 \pm 0.19 \pm 0.06$, respectively.

PACS numbers: 13.25 Hw, 13.20 He

The $b \to s\ell^+\ell^-$ transition is a flavor-changing neutral current (FCNC) process, which, in the Standard Model (SM), proceeds at lowest order via either a Z/γ penguin diagram or a W^+W^- box diagram. Since their amplitudes may interfere with the contributions from non-SM particles [1], the transition can probe the presence of yet unobserved particles and processes. More specifically, the lepton forward-backward asymmetry (A_{FB}) and the differential branching fraction as functions of dilepton invariant mass ($M_{\ell\ell}$) in the decays $B \to K^*\ell^+\ell^-$ differ from the SM expectations in various extended models [2]. The former is largely insensitive to the theoretical uncertainties of the form factors describing the decay, and can hence provide a stringent experimental test of the SM. The latter has been so far determined only with a modest precision [3, 4]. It can be used to extract the information on the coefficients associated with the theoretical models as well.

In this paper, we report measurements of the differential branching fractions and the isospin asymmetries as functions of $q^2 = M^2_{\ell\ell}c^2$ for $B \to K^*\ell^+\ell^-$ and $B \to K\ell^+\ell^-$ decays. The K^* polarization and A_{FB} for $B \to K^*\ell^+\ell^-$ decays as functions of q^2 are presented as well. A data sample of 657 million $B\overline{B}$ pairs, corresponding to 605 fb^{-1}, collected with the Belle detector at the KEKB asymmetric-energy e^+e^- collider [5] is examined. The Belle detector is described in detail elsewhere [6].

We reconstruct $B \to K^{(*)}\ell^+\ell^-$ signal events in 10 final states: $K^+\pi^-$, $K^0_S\pi^+$, $K^+\pi^0$, K^+, and K^0_S for $K^{(*)}$ [7], combined with either electron or muon pairs. All charged tracks other than the $K^0_S \to \pi^+\pi^-$ daughters are required to be associated with the interaction point (IP). A track is identified as a K^+ (π^+) by combining information from the aerogel Cherenkov and time-of-flight subsystems with dE/dx measurements in the central drift chamber [8]. The kaon (pion) identification is more than 85% (89%) efficient while removing more than 92% (91%) of pions (kaons). For muon (electron) candidates, we use the lepton identification likelihood described in Ref. [8], which we denote by $\mathcal{R}_x$ (x denotes μ or e). We select $\mu^\pm$ candidates with $p_\mu > 0.7$ GeV/c and momentum-dependent $\mathcal{R}_\mu$ requirements that retain (93.4%$\pm$2.0%) of muons while removing (98.8%$\pm$0.2%) of pions. Electron candidates are required to have $\mathcal{R}_e > 0.9$, $\mathcal{R}_\mu < 0.8$, and $p_e > 0.4$ GeV/c. These requirements retain (92.3%$\pm$1.7%) of electrons while removing (99.7%$\pm$0.1%) of pions. Bremsstrahlung photons emitted by electrons are recovered by adding neutral clusters found within a 50 mrad cone along the electron direction. The cluster energies are required to be between 20 and 500 MeV.

Pairs of oppositely-charged tracks are used to reconstruct $K^0_S \to \pi^+\pi^-$ candidates. The invariant mass is required to lie within the range 483–513 MeV/c^2 ($\pm$5 times the K^0_S reconstructed-mass resolution). Other selection criteria are based on the distance and the direction of the K^0_S vertex and the distance of daughter tracks to the IP. For $\pi^0 \to \gamma\gamma$ candidates, a minimum photon energy of 50 MeV is required and the invariant mass must be in the range 115 MeV/$c^2 < M_{\gamma\gamma} <$ 152 MeV/c^2 ($\pm$3 times the π^0 reconstructed-mass resolution). Requirements on the photon energy asymmetry $|E^1_\gamma - E^2_\gamma|/(E^1_\gamma + E^2_\gamma) < 0.9$ and π^0 momentum $p_{\pi^0} > 200$ MeV/c suppress the combinatorial background.

B-meson candidates are reconstructed by combining a $K^{(*)}$ candidate and a pair of oppositely charged leptons, and selected using the beam-energy constrained mass $M_{\rm bc} \equiv \sqrt{E^2_{\rm beam} - p^2_B}$ and the energy difference $\Delta E \equiv E_B - E_{\rm beam}$, where E_B and p_B are the reconstructed energy and momentum of the B candidate in the $\Upsilon(4S)$ rest frame and $E_{\rm beam}$ is the beam energy in this frame. Bremsstrahlung photons are included in the calculation of the momenta of electrons and hence are included in the calculations of $M_{\rm bc}$, $E_{\rm beam}$ and q^2. We require B-meson candidates to be within the region $M_{\rm bc} > 5.20$ GeV/c^2 and -35 (-55) MeV $< \Delta E <$ 35 MeV for the muon (electron) modes. The signal region is defined as

5.27 GeV/c^2 < $M_{\rm bc}$ < 5.29 GeV/c^2. For the K^* modes, the $M_{K\pi}$ candidate (signal) region is defined as $M_{K\pi}$ < 1.2 GeV/c^2 ($|M_{K\pi} - m_{K^*}|$ < 80 MeV/c^2).

The main backgrounds are continuum $e^+e^- \to q\overline{q}$ ($q = u, d, c, s$) and semileptonic B decay events. We use the same set of variables and the likelihood ratio, $\mathcal{R}$, described in Ref. [9], for continuum $e^+e^- \to q\overline{q}$ suppression. For the suppression of semileptonic B decays, we combine a Fisher discriminant including 16 modified Fox-Wolfram moments [10], the missing mass $M_{\rm miss} \equiv \sqrt{E^2_{\rm miss} - p^2_{\rm miss}}$, $\cos\theta_B$, and the lepton separation near the IP in the z direction to form the likelihood ratio $\mathcal{R}_{\rm sl} = \mathcal{L}_{\rm s}/(\mathcal{L}_{\rm s} + \mathcal{L}_{\rm sl})$, where $E_{\rm miss}(p_{\rm miss})$ is the missing energy (momentum), θ_B is the polar angle between the reconstructed B candidate and the beam direction in the $\Upsilon(4S)$ rest frame, and $\mathcal{L}_{\rm s}$ ($\mathcal{L}_{\rm sl}$) is the likelihood for signal (semileptonic B) decays. Combinatorial background suppression is improved by including q^2 and B-flavor tagging information [11]. Selection criteria for $\mathcal{R}$ and $\mathcal{R}_{\rm sl}$ are determined by maximizing the value of $S/\sqrt{S+B}$, where S and B denote the expected yields of signal and background events in the signal region, respectively, in different q^2 and tagging regions.

The dominant backgrounds that peak in the signal region are from $B \to J/\psi X$ and $\psi' X$ and rejected in the following q^2 regions (in units of GeV^2/c^2): 8.68 < $q^2(\mu^+\mu^-)$ < 10.09, 12.86 < $q^2(\mu^+\mu^-)$ < 14.18, 8.11 < $q^2(e^+e^-)$ < 10.03, and 12.15 < $q^2(e^+e^-)$ < 14.11. To remove the background from $B \to J/\psi(\psi')K^*$ events with one of the muons misidentified as a pion candidate, we reject events with -0.10 GeV/c^2 < $M_{\pi\mu} - m_{J/\psi(\psi')}$ < 0.08 GeV/c^2, where the pion is assigned the muon mass. Background from $B \to DX$ is rejected by additional veto windows $|M_{K\mu} - m_D|$ < 0.02 GeV/c^2 and $|M_{K\pi\mu} - m_D|$ < 0.02 GeV/c^2, where the muon is assigned the pion mass. The invariant mass of an electron pair must exceed 0.14 GeV/c^2 in order to remove background from photon conversions and $\pi^0 \to \gamma e^+e^-$ decays.

If multiple B candidates survive these selections in an event, we select the one with the smallest $|\Delta E|$. The fractions of multiple B events are about 7%, 12%, and 20% for the $K^+\pi^-$, $K^0_S\pi^+$, and $K^+\pi^0$ modes, respectively, and less than 1% for the K^+ and K^0_S modes, according to a study using Monte Carlo (MC) simulation of $B \to K^{(*)}\ell\ell$ decays.

To determine the signal yields, we perform an extended unbinned maximum likelihood fit to $M_{\rm bc}$ and $M_{K\pi}$ for $B \to K^*\ell^+\ell^-$ decays, and to $M_{\rm bc}$ for $B \to K\ell^+\ell^-$ decays. The likelihood function includes contributions from signal, combinatorial, $B \to J/\psi(\psi')X$, and $B \to K^{(*)}\pi\pi$ backgrounds. The signal PDFs consist of a Gaussian (Crystal Ball function [12]) in $M_{\rm bc}$ for the muon (electron) modes and a relativistic Breit-Wigner shape in $M_{K\pi}$ for the K^* resonance. The means and widths are determined from MC simulation and calibrated using $B \to J/\psi K^{(*)}$ decays. The PDFs of signal decays in which either the kaon or the pion candidate is wrongly associated to the K^* decay (self-cross-feed) are modelled by a two-dimensional smoothed histogram function with q^2-dependent fractions obtained from MC simulation of the signal decays. The combinatorial PDFs are represented by the product of an empirical ARGUS function [13] in $M_{\rm bc}$ with the sum in $M_{K\pi}$ of a threshold function (whose threshold is fixed at $m_K + m_\pi$) and a relativistic Breit-Wigner shape at the K^* resonance. The PDFs and yields for $B \to J/\psi(\psi')X$ decays are determined from a large MC sample, while the $B \to K^{(*)}\pi\pi$ PDFs and normalizations are determined from data, taking into account the probabilities of pions to be misidentified as muons. Yields for signal and combinatorial background and the combinatorial PDF parameters are allowed to float in the fit, while the yields and parameters for other components are fixed.

We divide q^2 into 6 bins and extract the signal and combinatorial background yields in each bin. The K^* longitudinal polarization fractions (F_L) and A_{FB} are extracted from fits to $\cos\theta_{K^*}$ and $\cos\theta_{B\ell}$, respectively, in the signal region, where θ_{K^*} is the angle between the

kaon direction and the direction opposite to the B meson in the K^* rest frame, and $\theta_{B\ell}$ is the angle between the ℓ^+ (ℓ^-) and the opposite of the B ($\overline{B}$) direction in the dilepton rest frame. The signal PDFs for the fit to $\cos\theta_{K^*}$ and $\cos\theta_{B\ell}$ are described by a product of the K^*/dilepton polarization function and the efficiency,

$$[\ \tfrac{3}{2}F_L\cos^2\theta_{K^*} + \tfrac{3}{4}(1-F_L)(1-\cos^2\theta_{K^*})\ ]\ \times\epsilon(\cos\theta_{K^*})$$

and

$$[\ \tfrac{3}{4}F_L(1-\cos^2\theta_{B\ell}) + \tfrac{3}{8}(1-F_L)(1+\cos^2\theta_{B\ell}) + A_{FB}\cos\theta_{B\ell}\ ]\times\epsilon(\cos\theta_{B\ell})\ ,$$

respectively. The first two terms in the dilepton polarization function correspond to the production of K^*'s with longitudinal and transverse polarization, while the third term generates the forward-backward asymmetry. Figures in Ref. [14] illustrate the fits for B yields, F_L, and A_{FB} in each q^2 bin. In the fit to $\cos\theta_{K^*}$ ($\cos\theta_{B\ell}$), F_L (A_{FB}) is the only free parameter, while the other PDFs and normalizations are fixed. For the $B\to K\ell^+\ell^-$ modes, we set $F_L=1$ and the $B\to K^0_S\ell^+\ell^-$ sample is not used.

TABLE I: Fit results in each of six q^2 bins and an additional bin from 1 to 6 GeV$^2/c^2$ for which recent theory predictions are available [15]. The first uncertainties are statistical and the second are systematic.

q^2 (GeV$^2/c^2$)	N_s	$\mathcal{B}(10^{-7})$	F_L	A_{FB}	A_I
			$B\to K^*\ell^+\ell^-$		
0.00–2.00	$27.4^{+7.4}_{-6.6}$	$1.46^{+0.40}_{-0.35}\pm0.11$	$0.29^{+0.21}_{-0.18}\pm0.02$	$0.47^{+0.26}_{-0.32}\pm0.03$	$-0.67^{+0.18}_{-0.16}\pm0.05$
2.00–4.30	$16.8^{+6.1}_{-5.3}$	$0.86^{+0.31}_{-0.27}\pm0.07$	$0.71^{+0.24}_{-0.24}\pm0.05$	$0.11^{+0.31}_{-0.36}\pm0.07$	$1.45^{+1.04}_{-1.15}\pm0.10$
4.30–8.68	$27.9^{+9.5}_{-8.5}$	$1.37^{+0.47}_{-0.42}\pm0.39$	$0.64^{+0.23}_{-0.24}\pm0.07$	$0.45^{+0.15}_{-0.21}\pm0.15$	$-0.34^{+0.29}_{-0.27}\pm0.14$
10.09–12.86	$54.0^{+10.5}_{-9.6}$	$2.24^{+0.44}_{-0.40}\pm0.19$	$0.17^{+0.17}_{-0.15}\pm0.03$	$0.43^{+0.18}_{-0.20}\pm0.03$	$0.00^{+0.20}_{-0.21}\pm0.09$
14.18–16.00	$36.2^{+9.9}_{-8.8}$	$1.05^{+0.29}_{-0.26}\pm0.08$	$-0.15^{+0.27}_{-0.23}\pm0.07$	$0.70^{+0.16}_{-0.22}\pm0.10$	$0.16^{+0.30}_{-0.35}\pm0.09$
>16.00	$84.4^{+11.0}_{-9.9}$	$2.04^{+0.27}_{-0.24}\pm0.16$	$0.12^{+0.15}_{-0.13}\pm0.02$	$0.66^{+0.11}_{-0.16}\pm0.04$	$-0.02^{+0.20}_{-0.21}\pm0.09$
1.00–6.00	$29.42^{+8.9}_{-8.0}$	$1.49^{+0.45}_{-0.40}\pm0.12$	$0.67^{+0.23}_{-0.23}\pm0.05$	$0.26^{+0.27}_{-0.30}\pm0.07$	$0.33^{+0.37}_{-0.43}\pm0.08$
			$B\to K\ell^+\ell^-$		
0.00–2.00	$27.0^{+6.0}_{-5.4}$	$0.81^{+0.18}_{-0.16}\pm0.05$	–	$0.06^{+0.32}_{-0.35}\pm0.02$	$-0.33^{+0.33}_{-0.25}\pm0.08$
2.00–4.30	$17.6^{+5.5}_{-4.8}$	$0.46^{+0.14}_{-0.12}\pm0.03$	–	$-0.43^{+0.38}_{-0.40}\pm0.09$	$-0.47^{+0.50}_{-0.38}\pm0.07$
4.30–8.68	$39.1^{+7.5}_{-6.9}$	$1.00^{+0.19}_{-0.18}\pm0.06$	–	$-0.20^{+0.12}_{-0.14}\pm0.03$	$-0.19^{+0.25}_{-0.21}\pm0.08$
10.09–12.86	$22.0^{+6.2}_{-5.5}$	$0.55^{+0.16}_{-0.14}\pm0.03$	–	$-0.21^{+0.17}_{-0.15}\pm0.06$	$-0.29^{+0.37}_{-0.29}\pm0.08$
14.18–16.00	$15.6^{+4.9}_{-4.3}$	$0.38^{+0.19}_{-0.12}\pm0.02$	–	$0.04^{+0.32}_{-0.26}\pm0.05$	$-0.40^{+0.61}_{-0.69}\pm0.07$
>16.00	$40.3^{+8.2}_{-7.5}$	$0.98^{+0.20}_{-0.18}\pm0.06$	–	$0.02^{+0.11}_{-0.08}\pm0.02$	$0.11^{+0.24}_{-0.21}\pm0.08$
1.00–6.00	$52.0^{+8.7}_{-8.0}$	$1.36^{+0.23}_{-0.21}\pm0.08$	–	$-0.04^{+0.13}_{-0.16}\pm0.05$	$-0.41^{+0.25}_{-0.20}\pm0.07$

Table I lists the measurements of B yields; the partial branching fractions, obtained by correcting the B yields for q^2-dependent efficiencies; F_L; and A_{FB} in individual q^2 bins. In the calculation of the partial branching fractions, we adopt the SM lepton flavor ratios of

the muon to electron modes [16] and express the branching fractions in terms of the muon channel. The ratio for the full q^2 interval is $R_{K^*}^{\rm SM} = 0.75$ ($R_K^{\rm SM} = 1$) for the $B \to K^*\ell^+\ell^-$ ($B \to K\ell^+\ell^-$) mode, where the deviation from unity is due to the photon pole. The results, as well as the SM curves, are shown in Fig. 1. To illustrate how non-SM physics might manifest itself, we superimpose curves on the F_L and A_{FB} plots corresponding to the case of C_7 with reversed sign ($C_7 = -C_7^{SM}$). The measured values do not reject this possibility.

The total branching fractions, extrapolated from the partial branching fractions, are measured to be [17]

$$\begin{aligned} \mathcal{B}(B \to K^*\ell^+\ell^-) &= (10.7^{+1.1}_{-1.0} \pm 0.9) \times 10^{-7} \ , \\ \mathcal{B}(B \to K\ell^+\ell^-) &= (4.8^{+0.5}_{-0.4} \pm 0.3) \times 10^{-7} \ ; \end{aligned}$$

while the fitted CP asymmetries, defined in terms of the $\overline{B}$ (B) yield N_b ($N_{\bar{b}}$) as $A_{CP} \equiv (N_b - N_{\bar{b}})/(N_b + N_{\bar{b}})$, are [14]

$$\begin{aligned} A_{CP}(K^*\ell^+\ell^-) &= -0.10 \pm 0.10 \pm 0.01 \ , \\ A_{CP}(K^+\ell^+\ell^-) &= 0.04 \pm 0.10 \pm 0.02 \ . \end{aligned}$$

The lepton flavor ratio is sensitive to Higgs emission and is predicted to be larger than the SM value in the Higgs doublet model at large $\tan\beta$ [18]. The measured ratios are

$$\begin{aligned} R_{K^*} &= 0.83 \pm 0.17 \pm 0.08 \ , \\ R_K &= 1.03 \pm 0.19 \pm 0.06 \ . \end{aligned}$$

The isospin asymmetry, shown in Table I and Fig. 1, is defined as

$$A_I \equiv \frac{(\tau_{B^+}/\tau_{B^0}) \times \mathcal{B}(K^{(*)0}\ell^+\ell^-) - \mathcal{B}(K^{(*)\pm}\ell^+\ell^-)}{(\tau_{B^+}/\tau_{B^0}) \times \mathcal{B}(K^{(*)0}\ell^+\ell^-) + \mathcal{B}(K^{(*)\pm}\ell^+\ell^-)} \ ,$$

where $\tau_{B^+}/\tau_{B^0} = 1.071$ is the lifetime ratio of B^+ to B^0 [19]. A large isospin asymmetry for q^2 below the mass of the J/ψ resonance was reported recently [20]. We also measure the combined A_I for $q^2 < 8.68$ GeV$^2/c^2$ and find

$$\begin{aligned} A_I(B \to K^*\ell^+\ell^-) &= -0.29^{+0.16}_{-0.16} \pm 0.09 \quad \sigma = 1.37 \ , \\ A_I(B \to K\ell^+\ell^-) &= -0.31^{+0.17}_{-0.14} \pm 0.08 \quad \sigma = 1.75 \ , \\ A_I(B \to K^{(*)}\ell^+\ell^-) &= -0.30^{+0.12}_{-0.11} \pm 0.08 \quad \sigma = 2.22 \ , \end{aligned}$$

where σ denotes the significance from a null asymmetry and is defined as $\sigma \equiv \sqrt{-2\ln(\mathcal{L}_0/\mathcal{L}_{\rm max})}$, where $\mathcal{L}_0$ is the likelihood with A_I constrained to be zero and $\mathcal{L}_{\rm max}$ is the maximum likelihood. Systematic uncertainties are considered in the significance calculation. No significant isospin asymmetry is found at low q^2.

Systematic uncertainties in the branching fraction measurements arise predominantly from tracking efficiencies (2.0%–4.4%), MC decay models (0.9%–4.6%), electron (3.0%) and muon (2.6%) identification, K_S^0 (4.9%) and π^0 (4.0%) reconstruction, and $\mathcal{R}$ and $\mathcal{R}_{\rm sl}$ selection (1.2%–3.6%). The MC simulated samples of the signal are generated based on a model derived from Ref. [16]. The modeling uncertainties are evaluated by comparing MC samples based on different models [21], while lepton identification is studied using a $J/\psi \to \ell^+\ell^-$ data sample. For $\mathcal{R}$ and $\mathcal{R}_{\rm sl}$ selections, we estimate the uncertainties from large control samples

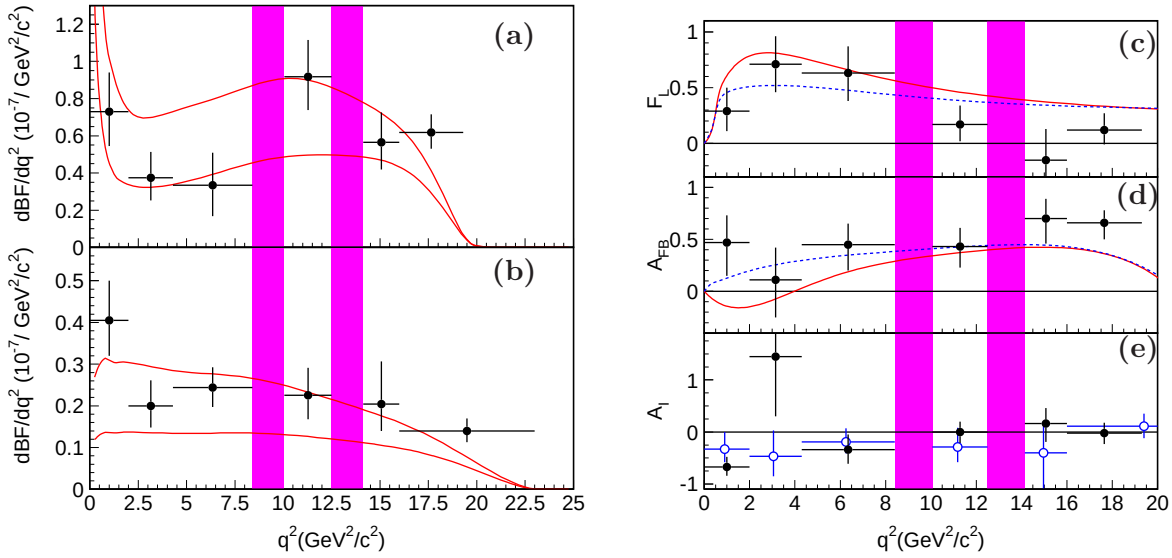

FIG. 1: Differential branching fractions for the (a) $K^*\ell^+\ell^-$ and (b) $K\ell^+\ell^-$ modes as a function of q^2. The two shaded regions are veto windows to reject $J/\psi(\psi')X$ events. The solid curves show the SM theoretical predictions with the minimum and maximum allowed form factors [16]. (c) and (d) show the fit results for F_L and A_{FB} in $K^*\ell^+\ell^-$ as a function of q^2, together with the solid (dotted) curve representing the SM ($C_7 = -C_7^{SM}$) prediction [16]. (e) is the A_I asymmetry as a function of q^2 for the $K^*\ell^+\ell^-$ (filled circles) and $K\ell^+\ell^-$ (open circles) modes.

with the same final states, $B \to J/\psi K^{(*)}$ with $J/\psi \to \ell^+\ell^-$. Other uncertainties such as kaon and pion identification efficiencies, fitting PDFs, background contamination from J/ψ decays and charmless B decays, and the number of $B\overline{B}$ pairs are found to be small. The total systematic uncertainties in the branching fractions for different decay channels are 6.8%–12.2% and 5.2%–7.4% for the $K^*\ell^+\ell^-$ and $K\ell^+\ell^-$ modes, respectively.

The main uncertainties for angular fits are propagated from the errors on the fixed normalizations and F_L, determined from $M_{\rm bc}$–$M_{K\pi}$ and $\cos\theta_{K^*}$ fits, respectively. Fitting bias and fitting PDFs are checked using large $B \to J/\psi K^{(*)}$ and MC samples. The total uncertainties for the F_L and A_{FB} fits depend on the q^2 bin and range from 0.02–0.06 and 0.03–0.13, respectively. The systematic errors on A_{CP} are assigned using the CP asymmetry measured in sideband data without $\mathcal{R}$ and $\mathcal{R}_{\rm sl}$ selections and are found to be 0.01–0.02. The systematic error on $R_{K^{(*)}}$ (A_I) is determined by combining the uncertainties from lepton (K/π) identification, $\mathcal{R}$ and $\mathcal{R}_{\rm sl}$ selections, fitting PDFs and background contamination. The uncertainty in A_I from the assumption of equal production of $B^0\bar{B}^0$ and B^+B^- pairs is also considered. The correlated systematic errors among q^2 bins are negligible for all the measurements.

In summary, we report the differential branching fraction, isospin asymmetry, K^* longitudinal polarization and forward-backward asymmetry as functions of q^2, as well as total branching fractions, lepton flavor ratios, and CP asymmetries for $B \to K^{(*)}\ell^+\ell^-$. These results supersede our previous measurements [3] and are consistent with the latest BaBar results [4, 20] with better precision. The differential branching fraction, lepton flavor ratios, and K^* polarization are consistent with the SM predictions. No significant CP asymmetry is found in the study. The isospin asymmetry does not deviate significantly from the null value. The $A_{FB}(q^2)$ spectrum for $B \to K^*\ell^+\ell^-$ decays tends to be shifted toward the pos-

itive side from the SM expectation. The cumulative difference between the SM prediction and the measured points is found to be 2.7 standard deviations. A much larger data set, which will be available at the proposed super B factory [22] and LHCb [23], is needed to make more precise tests of the SM.

We thank the KEKB group for excellent operation of the accelerator, the KEK cryogenics group for efficient solenoid operations, and the KEK computer group and the NII for valuable computing and SINET3 network support. We acknowledge support from MEXT, JSPS and Nagoya's TLPRC (Japan); ARC and DIISR (Australia); NSFC (China); DST (India); MOEHRD and KOSEF (Korea); MNiSW (Poland); MES and RFAAE (Russia); ARRS (Slovenia); SNSF (Switzerland); NSC and MOE (Taiwan); and DOE (USA).

[1] S. Davidson, D. C. Bailey and B. A. Campbell, Z. Phys. C **61**, 613 (1994); G. Burdman, Phys. Rev. D **52**, 6400 (1995); J. L. Hewett and J. D. Wells, Phys. Rev. D **55**, 5549 (1997).

[2] F. Kruger, L. M. Sehgal, N. Sinha and R. Sinha, Phys. Rev. D **61**, 114028 (2000) [Erratum-ibid. D **63**, 019901 (2001)]; A. Ali, E. Lunghi, C. Greub and G. Hiller, Phys. Rev. D **66**, 034002 (2002); T. M. Aliev, A. Ozpineci and M. Savci, Eur. Phys. J. C **29**, 265 (2003) and references therein; W. S. Hou, A. Hovhannisyan and N. Mahajan, Phys. Rev. D **77**, 014016 (2008).

[3] A. Ishikawa *et al.* (Belle Collaboration), Phys. Rev. Lett. **91**, 261601 (2003); A. Ishikawa *et al.* (Belle Collaboration), Phys. Rev. Lett. **96**, 251801 (2006).

[4] B. Aubert *et al.* (BaBar Collaboration), Phys. Rev. D **73**, 092001 (2006); B. Aubert *et al.* (BaBar Collaboration), Phys. Rev. D **79**, 031102 (2009).

[5] S. Kurokawa and E. Kikutani, Nucl. Instrum. Methods Phys. Res., Sect. A **499**, 1 (2003) and other papers included in this Volume.

[6] A. Abashian *et al.* (Belle Collaboration), Nucl. Instrum. Methods Phys. Res., Sect. A **479**, 117 (2002).

[7] Charge-conjugate decays are implied and equal production of $B^0\overline{B}^0$ and B^+B^- pairs is assumed throughout the paper.

[8] E. Nakano, Nucl. Instrum. Methods Phys. Res., Sect. A **494**, 402 (2002).

[9] J.-T. Wei *et al.* (Belle Collaboration), Phys. Rev. D **78**, 011101(R) (2008).

[10] G. C. Fox and S. Wolfram, Phys. Rev. Lett. **41**, 1581 (1978).

[11] H. Kakuno *et al.*, Nucl. Instrum. Methods Phys. Res., Sect. A **533**, 516 (2004).

[12] T. Skwarnicki (Crystal Ball Collaboration), Ph.D. thesis, Cracow Institute of Nuclear Physics, DESY F31-86-02 (1986).

[13] H. Albrecht *et al.* (ARGUS Collaboration), Phys. Lett. B **185**, 218 (1987).

[14] See EPAPS supplementary material at [URL will be inserted by AIP] for fit figures, as well as the total branching fractions and CP asymmetries for individual $K^{(*)}\ell^+\ell^-$ modes.

[15] M. Beneke, Th. Feldmann and D. Seidel, Eur. Phys. J. C **41**, 173 (2005); C. Bobeth, G. Hiller and G. Piranishvili, JHEP **0712**, 040 (2007).

[16] A. Ali, P. Ball, L. T. Handoko and G. Hiller, Phys. Rev. D **61**, 074024 (2000). A. Ali, E. Lunghi, C. Greub and G. Hiller, Phys. Rev. D **66**, 034002 (2002);

[17] The first and second errors are statistical and systematic, respectively, in all measurements quoted throughout the paper.

[18] Y. Wang and D. Atwood, Phys. Rev. D **68**, 094016 (2003).

[19] C. Amsler *et al.* (Particle Data Group), Phys. Lett. B **667**, 1 (2008).
[20] B. Aubert *et al.* (BaBar Collaboration), Phys. Rev. Lett. **102**, 091803 (2009).
[21] D. Melikhov, N. Nikitin and S. Simula, Phys. Lett. B **410**, 290 (1997); P. Colangelo, F. De-Fazio, P. Santorelli and E. Scrimieri, Phys. Rev. D **53**, 3672 (1996).
[22] A. G. Akeroyd *et al.* (The SuperKEKB Physics Working Group), arXiv:hep-ex/0406071.
[23] J. Dickens (LHCb Collaboration), CERN-LHCb-2007-038.

APPENDIX

Below is EPAPS supplementary material for fit figures, as well as the total branching fractions and CP asymmetries for individual $K^{(*)}\ell^+\ell^-$ modes, which is mentioned in Ref. [14].

TABLE II: Total branching fractions and CP asymmetries for subsamples of $B \to K^*\ell^+\ell^-$ and $B \to K\ell^+\ell^-$ decays.

Mode	$\mathcal{B}$ (10^{-7})	A_{CP}
$K^{*+}\mu^+\mu^-$	$11.1^{+3.2}_{-2.7}\pm1.0$	$-0.12^{+0.24}_{-0.24}\pm0.02$
$K^{*0}\mu^+\mu^-$	$10.6^{+1.9}_{-1.4}\pm0.7$	$0.00^{+0.15}_{-0.15}\pm0.03$
$K^*\mu^+\mu^-$	$11.0^{+1.6}_{-1.4}\pm0.8$	$-0.03^{+0.13}_{-0.13}\pm0.02$
$K^{*+}e^+e^-$	$17.3^{+5.0}_{-4.2}\pm2.0$	$-0.14^{+0.23}_{-0.22}\pm0.02$
$K^{*0}e^+e^-$	$11.8^{+2.7}_{-2.2}\pm0.9$	$-0.21^{+0.19}_{-0.19}\pm0.02$
$K^*e^+e^-$	$13.9^{+2.3}_{-2.0}\pm1.2$	$-0.18^{+0.15}_{-0.15}\pm0.01$
$K^{*+}\ell^+\ell^-$	$12.4^{+2.3}_{-2.1}\pm1.3$	$-0.13^{+0.17}_{-0.16}\pm0.01$
$K^{*0}\ell^+\ell^-$	$9.7^{+1.3}_{-1.1}\pm0.7$	$-0.08^{+0.12}_{-0.12}\pm0.02$
$K^*\ell^+\ell^-$	$10.7^{+1.1}_{-1.0}\pm0.9$	$-0.10^{+0.10}_{-0.10}\pm0.01$
$K^+\mu^+\mu^-$	$5.3^{+0.8}_{-0.7}\pm0.3$	$-0.05^{+0.13}_{-0.13}\pm0.03$
$K^0\mu^+\mu^-$	$4.4^{+1.3}_{-1.1}\pm0.3$	–
$K\mu^+\mu^-$	$5.0^{+0.6}_{-0.6}\pm0.3$	–
$K^+e^+e^-$	$5.7^{+0.9}_{-0.8}\pm0.3$	$0.14^{+0.14}_{-0.14}\pm0.03$
$K^0e^+e^-$	$2.0^{+1.4}_{-1.0}\pm0.1$	–
Ke^+e^-	$4.8^{+0.8}_{-0.7}\pm0.3$	–
$K^+\ell^+\ell^-$	$5.3^{+0.6}_{-0.5}\pm0.3$	$0.04^{+0.10}_{-0.10}\pm0.02$
$K^0\ell^+\ell^-$	$3.4^{+0.9}_{-0.8}\pm0.2$	–
$K\ell^+\ell^-$	$4.8^{+0.5}_{-0.4}\pm0.3$	–

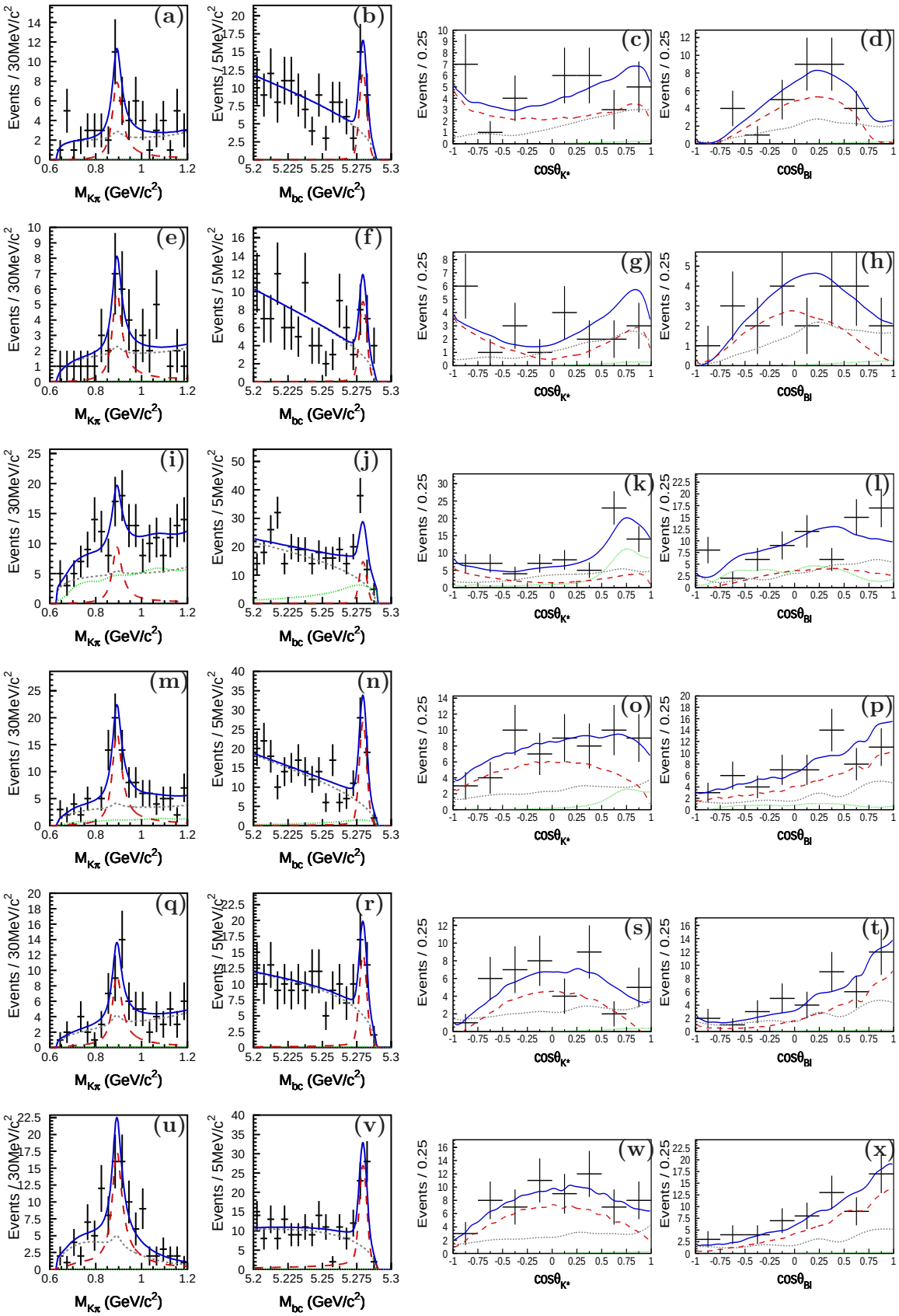

FIG. 2: Fits to $M_{K\pi}$, $M_{\rm bc}$, $\cos\theta_{K^*}$, and $\cos\theta_{B\ell}$ for the $K^*\ell^+\ell^-$ decays in 6 q^2 (GeV$^2/c^2$) bins: (a)$\sim$(d) 0.00–2.00, (e)$\sim$(h) 2.00–4.30, (i)$\sim$(l) 4.30–8.68, (m)$\sim$(p) 10.09–12.86, (q)$\sim$(t) 14.18–16.00, and (u)$\sim$(x) $>$ 16.00. The solid, long-dashed, short-dashed, and dotted curves represent the combined fit result, fitted signal, combinatorial background, and $J/\psi(\psi')X$ background, respectively.

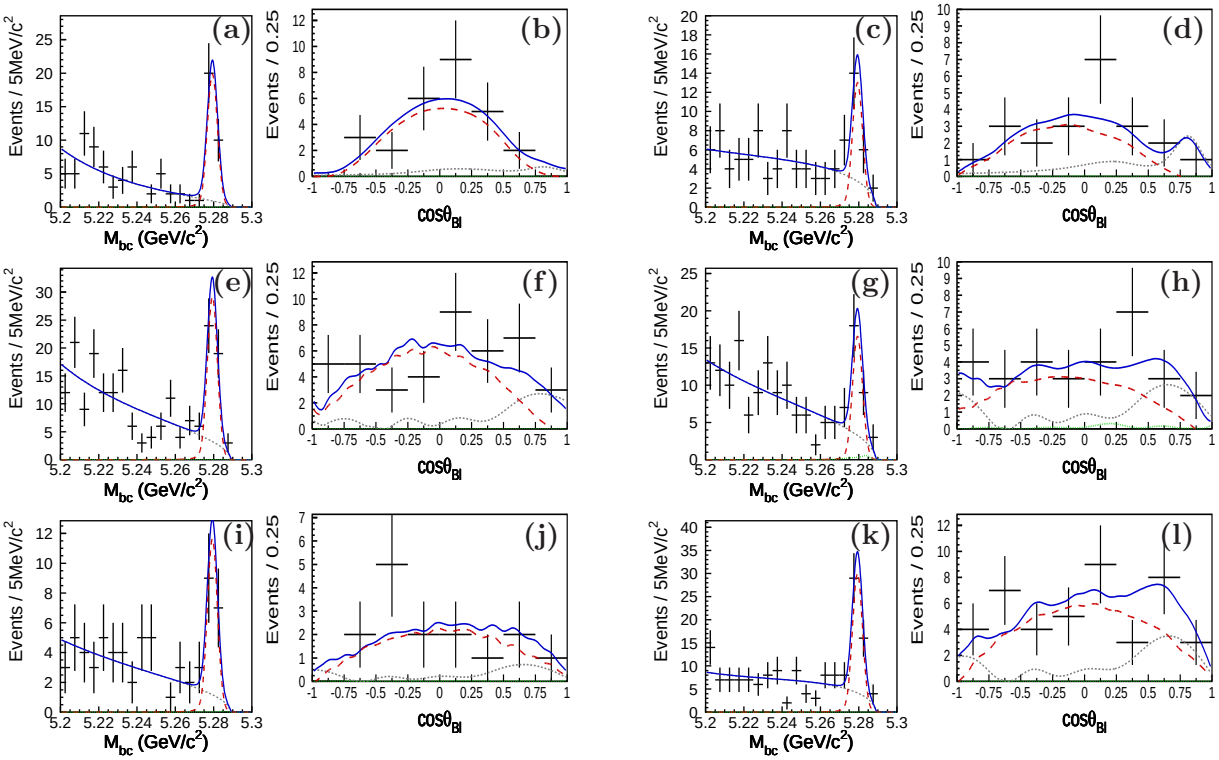

FIG. 3: Fits to $M_{\rm bc}$ and $\cos\theta_{B\ell}$ for the $K\ell^+\ell^-$ decays in 6 q^2 (GeV$^2/c^2$) bins: (a)$\sim$(b) 0.00–2.00, (c)$\sim$(d) 2.00–4.30, (e)$\sim$(f) 4.30–8.68, (g)$\sim$(h) 10.09–12.86, (i)$\sim$(j) 14.18–16.00, and (k)$\sim$(l) $>$ 16.00. The solid, long-dashed, and short-dashed represent the combined fit result, fitted signal, and combinatorial background, respectively. The$J/\psi(\psi')X$ background is so small and not represented.